Enhancing the Structural Performance of Additively Manufactured Objects Through Build Orientation Optimization

Erva Ulu, Emrullah Korkmaz, Kubilay Yay, O. Burak Ozdoganlar, Levent Burak Kara*
Department of Mechanical Engineering,
Carnegie Mellon University,
Pittsburgh, PA 15213
e-mail: lkara@cmu.edu

Additively manufactured objects often exhibit directional dependencies in their structure due to the layered nature of the printing process. While this dependency has a significant impact the object's functional performance, the problem of finding the best build orientation to maximize structural robustness remains largely unsolved. We introduce an optimization algorithm that addresses this issue by identifying the build orientation that maximizes the factor of safety of an input object under prescribed loading and boundary configurations. First, we conduct a minimal number of physical experiments to characterize the anisotropic material properties. Next, we use a surrogate-based optimization method to determine the build orientation that maximizes the minimum factor safety. The surrogate-based optimization starts with a small number of finite element solutions corresponding to different build orientations. The initial solutions are progressively improved with the addition of new solutions until the optimum orientation is computed. We demonstrate our method with physical experiments on various test models from different categories. We evaluate the advantages and limitations of our method by comparing the failure characteristics of parts printed in different orientations.

1 Introduction

There is a growing interest in additive manufacturing (AM) due to its applicability to complex geometries, rapid design-to-fabrication turnaround, and its widening spectrum of material choice, making it suitable in a myriad of engineering applications [1–6]. In the context of structural and geometric design, recent works have investigated automatic techniques to achieve prescribed functions such as designing for desired deformations [7, 8], designing for prescribed appearances [9, 10], balancing models [11] and generating spinnable objects [12].

The *layered* nature of AM has major implications on the resulting objects. To date, there have been many studies highlighting the impact of build orientation (*i.e.,* how the part is oriented in the print workspace) on aspects such as surface quality, the amount of required support material, geometric accuracy, build time, and overall fabrication cost [13–16]. However, the build orientation has a major impact on the structural properties of additively manufactured parts. This is commonly manifested in the form of anisotropically printed objects, making structural performance highly dependent on the build orientation. While this intricacy has been observed and experimentally demonstrated in a limited fashion, to date, no attempts have been made to engineer its impact to improve structural robustness.

In this work, we introduce a new build orientation selection algorithm for polymer-based AM processes that aims to maximize an input object's resistance to failure under prescribed external loads. We define an increased resistance to failure as one that increases the direction-dependent material yield strength relative to the stresses generated within the object. We thus formulate a new build orientation optimization problem where the optimal orientation is achieved by maximizing the minimum factor of safety observed in the object. The problem, however, is difficult to solve using conventional gradient-based methods. This is because the build orientation impacts several structural parameters including the elastic moduli, the yield strengths, and the material's Poisson's ratios. Additionally, unless the domain is particularly simple, where appropriate analytical functions can be utilized, the relationship between the build orientation and the resulting stress tensor field is difficult to establish in closed form. This difficulty makes the gradient and the Hessian of the objective function very difficult to precompute for arbitrary geometries and loading configurations.

On the other hand, a brute force approach (*e.g.,* uniform parameter sweep) will typically require a large number of finite element (FE) simulations to appropriately cover the design space, which can be computationally prohibitive. To address this challenge, we use a surrogate-based optimization method that starts with a small number of FE simulations for

*Address all correspondence to this author.

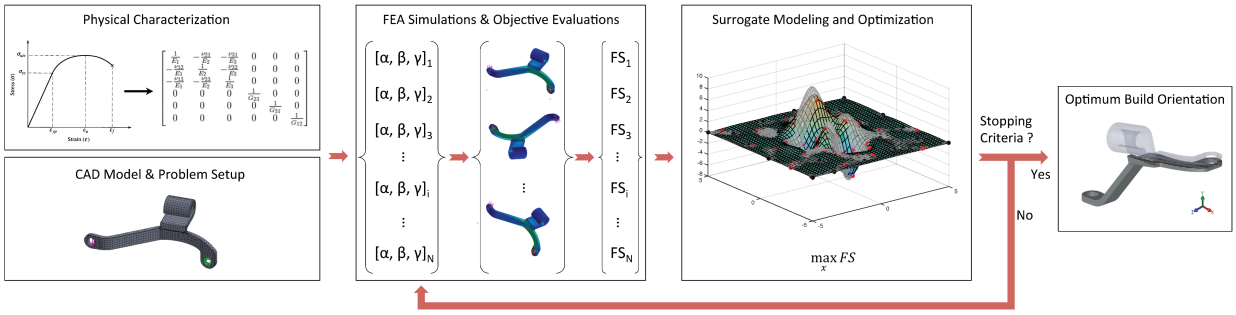

Fig. 1. Our approach takes as input a 3D model of an object with the corresponding loading/boundary configurations and anisotropic (orthotropic) material properties, then calculates an optimum build orientation that maximizes the factor of safety (FS). The build orientation is defined by three Euler angles $[\alpha, \beta, \gamma]$. A surrogate model between the candidate orientations and the objective function is constructed. The surrogate model is progressively improved with the addition of new candidate orientations until the optimal orientation is found.

various build orientations to model the design space. Then, the initial surrogate model is iteratively improved with the addition of new evaluation points until the optimum orientation is found. In each iteration, the functional form of the surrogate model enables a gradient-based search on this proxy model, thereby accelerating the optimization process.

Our optimization algorithm uses an orthotropic material model to establish the compliance matrix. To identify the parameters of this matrix, we perform a set of physical experiments on a small set of test specimens that are printed using the target object's material and print settings (Fig. 1). This choice enables the process and environment dependent properties to be accounted for during our solutions.

Contributions. Our primary contributions are as follows:

1. A novel build orientation selection algorithm for AM that maximizes the minimum factor of safety under prescribed loading and boundary conditions.
2. A surrogate-based optimization approach that minimizes the number of FE simulations.
3. A framework to experimentally determine the process dependent anisotropic material properties.

2 Related Work

There is a growing interest in AM technologies in the fields of computational design, process design and material science. Here, we focus on the studies that highlight the *directional dependencies* in AM, computational design with *structural concerns* and *build orientation* selection for AM.

2.1 Directional Dependencies

The most commonly studied effects of print-induced anisotropy include dimensional accuracy and surface roughness [14, 17], build time and cost [15, 16], the amount of support material [13, 18] and the mechanical properties (*e.g.,* strength, elastic modulus) [19, 20]. Most relevant to our work, we focus on the studies examining the anisotropy in the structural properties of AM parts.

Various studies have experimentally shown that 3D printed parts exhibit directional dependencies in their mechanical properties. Ahn *et al.* [19] characterize the anisotropic mechanical properties of ABS parts manufactured using fused deposition modeling (FDM). Similarly, El-Gizawy *et al.* [21] and Hill and Haghi [22] investigate the mechanical properties of polyetherimide and polycarbonate when used in FDM. Barclift and Williams [23] and Kesy and Kotlinski [24] experimentally study the effects of process parameters on material properties in polyjet printing. Similarly, Galeta *et al.* [25] study powder based AM. These experimental studies demonstrate that AM induces a significant structural anisotropy for many process and material combinations. Moreover, these works have shown that the resulting anisotropy can be represented very well using an orthotropic material model.

Several computational methods have also been proposed to address this problem. Hildebrand *et al.* [26] minimize the directional bias by partitioning the model into parts and selecting a build direction individually for each part. However, they investigate the geometric accuracy only. Zhou *et al.* [27] take a worst-case analysis approach to identify the structurally weak parts of a design where a constrained optimization problem is solved to obtain the worst loading configuration with the orthotropic material assumption. Umetani and Schmidt [28] address the structural anisotropy in FDM with the assumption that the vertical bonds between the layers are much weaker than the in-layer bonds. Based on this assumption, a cross sectional heuristic analysis is formulated to find an orientation that maximizes mechanical strength. Our approach builds upon these prior works by enabling a orthotropic material model with unique properties in each of the three principal directions. Additionally, in our approach, we maximize the factor of safety by considering the prescribed external loads and boundary conditions without making simplifying assumptions about the analysis.

2.2 Structural Concerns

Several studies have recently focused on the computational design for AM addressing structural concerns. In these studies, a common approach is to deform or modify the initial design to overcome its structural problems. Luo *et al.* [29] partition large objects into 3D printable smaller parts where each partition's impact on the overall structural

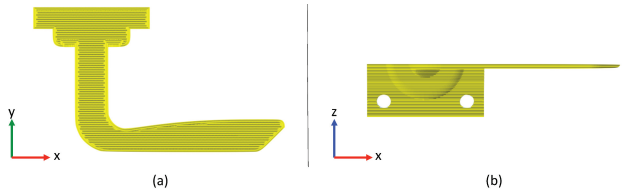

Fig. 2. Principal directions in the orthotropic material model (a) A single layer in AM process where x and y are the in-plane principal directions. (b) The layer accumulation (build) direction, z.

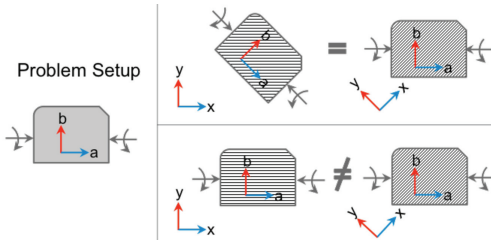

Fig. 3. Geometry a, b and material x, y coordinate frames. The top row shows an example for the equivalent representations of the same physical problem. The bottom row illustrates our case where there are two distinct build orientations and separate FE simulations are required to obtain the stress information for each configuration. Hence, while stress transformation formulas seem to be applicable here, they are indeed not applicable in our problem.

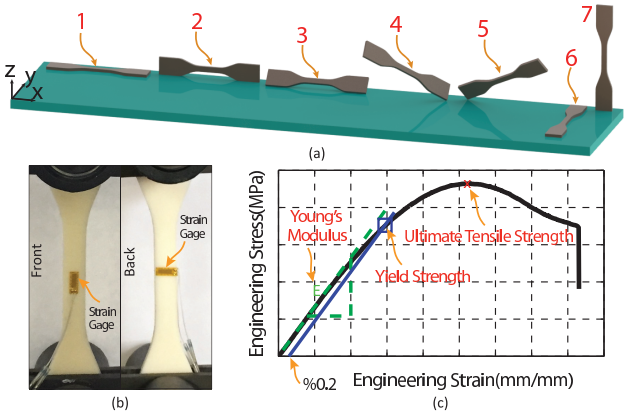

Fig. 4. Material characterization. (a) Print directions considered, (b) experimental setup for tensile tests and (c) a typical stress-strain curve showing a subset of the material properties to be extracted.

robustness is evaluated using FE analysis, which informs the strategy for subsequent partitions. Similarly, Stava *et al.* [30] evaluate hand-held objects' structural weakness using FE analysis to determine parts of the designs that require thickening, hollowing, or strut placement. Analysis is restricted to boundary conditions representing gravity and gripping using two fingers at heuristically predicted locations. Based on this analysis, several automatic shape modifications are proposed.

Recent works have also focused on cost-effective 3D printing strategies while still addressing structural concerns. Wang *et al.* [31] replace the solid interior of the object with a truss structure to reduce the amount of material used in the printing process. Lu *et al.* [32] use a hollowing approach based on Voronoi diagrams to obtain lightweighted structures that can sustain prescribed stresses.

In our approach, we preserve the input design and do not perform shape modification. Instead, for an input design with prescribed boundary conditions, we optimize the build orientation to maximize the stress-based factor of safety in the resulting fabricated object. However if needed, the above cost-effective methods can be used as a pre-processing step to reduce the amount of material used in AM.

2.3 Build Orientation

Although build orientation selection with respect to geometrical features is very well studied for AM applications, there is only a limited amount of work that directly addresses structural concerns. Suh and Wozny [33] account for the critical features (*e.g.,* thin walls and slender protrusions) that need to be appropriately oriented due to potential failure problems. They use a purely geometric approach to ensure that the critical features lie in the layer accumulation direction and do not consider the loading conditions on the designed object. In an inspiring work, Thompson and Crawford [34] introduce a build orientation selection algorithm that considers the load and boundary conditions together with the material properties. To this end, they use the Tsai-Wu failure criterion to determine whether the object is safe or unsafe for a candidate build orientation. However, this binary objective only ensures safe orientations and does not maximize the factor of safety. Umetani and Schmidt [28] suggest the best build orientation for a given geometry by analyzing the structural weakness at different cross-sections assuming that the primary mode of loading is bending. The part is oriented such that the weakest cross-sections are as perpendicular as possible to the layer accumulation direction. This approach assumes that the material behaves isotropically within a single layer, hence the in-layer orientation does not affect mechanical strength.

Our approach is inspired by the studies presented in [34] and [28] in that the actual loading conditions determine the build orientation if the structural robustness is the main concern. However, unlike [34], we maximize the mechanical strength over the entire geometry instead of incorporating the failure criterion as a constraint when assessing candidate orientations. Moreover, our work differs from [28] in that we do not assume in-layer isotropy and allow all modes of loading configurations (bending, torsion, compression *etc.*) to be jointly considered.

3 Preliminaries

We begin by introducing our material model, our FE simulation infrastructure and the techniques to physically characterize the anisotropy in 3D printed parts.

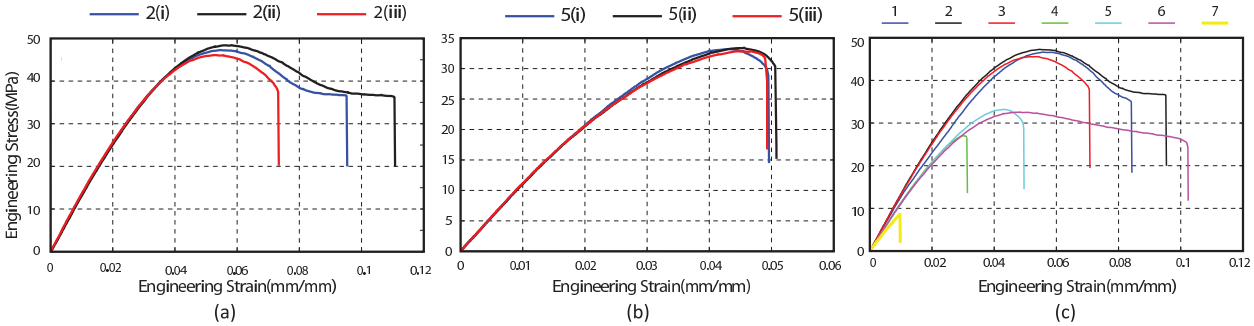

Fig. 5. Repeatability tests for (a) orientation 2, (b) orientation 5 and (c) the stress-strain curves for different build orientations shown in Fig. 4.

Table 1. Results of physical characterization tests for the three principal directions.

Principal Directions	Young's Modulus [GPa]	Yield Strength [MPa] (Tensile/Compressive)	Shear Modulus* [GPa]	Shear Strength [MPa]	Poisson's Ratio
x	1.16	35.86/52.46	0.51	4.38	0.09
y	1.05	25.52/37.63	0.28	4.38	0.37
z	0.52	8.77/13.58	0.30	4.38	0.31

* Determined analytically using [27].

3.1 Material Model and Analysis

We base our approach on an orthotropic material model which is commonly used in AM due to the 3-orthogonal nature of the print process. Figure 2 illustrates the three principal directions with the coordinate frame $x \perp y \perp z$. Here, x and y correspond to the orthogonal in-layer directions and z corresponds to the layer accumulation direction.

In the orthotropic material model, a total of nine parameters need to be determined experimentally. These parameters are the Young's moduli, shear moduli and Poisson's ratios for the three principal directions. Additionally, to compute the factor of safety, the tensile yield strength, compressive yield strength and shear strength need to be determined experimentally for these principal directions. The orthotropic material model enables all such parameters to be determined with a minimal number of tests using well established metrology techniques including tensile, compressive and shear tests. Further details of the material characterization experiments are explained in Section 3.3.

3.2 Finite Element Analysis

We use FE simulations to calculate the stress tensor field for a given geometry and boundary conditions. With the orthotropic material assumption, a new FE simulation is required for each candidate build orientation. Figure 3 illustrates this issue on a simple two dimensional example. For a given geometry and boundary conditions, we assign a local coordinate frame, $a \perp b$ ($\perp c$ for 3D), which is attached to the *geometry*. We also establish a global coordinate frame, $x \perp y$ ($\perp z$ for 3D) that represents the *material* orientation.

In this paper, we use a script based ANSYS Mechanical Parametric Design Language (APDL) to run FE simulations required in our optimization scheme. During optimization, a new material coordinate frame is established that operates on a fixed geometry, mesh, and boundary conditions. The different build orientations are thus evaluated by adjusting the material coordinate frame. After each FE simulation, the computed stress tensor information is encoded in the geometry coordinate frame, thus a stress transformation is required to evaluate the stress values in the material coordinate frame where the structural properties are known. This transformation facilitates the factor of safety calculation at each element in the domain as will be shown later.

3.3 Material Characterization

To demonstrate the integration of physical anisotropy characterization into our optimization scheme, we use a high-resolution (30μm vertical and 42μm lateral) Objet Connex 350 multi-material 3D printing system. Thin layers of photosensitive resins (30μm) are deposited onto a build tray (350 mm x 350 mm x 200 mm) by inkjet printing. The deposited layer is then immediately cured using a UV light source for photo-polymerization, which is coupled to the print head and solidifies each liquid material layer. During the curing process, a roller levels the liquid polymers making the material immediately ready to be built upon with successive layers. The building process uses two kinds of material: object (two different materials can be used and different digital materials can be obtained through a mixture of these materials) and support. It is possible to build the final product with and without the support material around the features.

Using this setup, we print a test specimen in seven different orientations and perform a tensile test for each orientation to reveal the directional dependency of the material properties (Fig. 4). For each direction, we print three copies of ASTM D638 standard tensile test specimen using

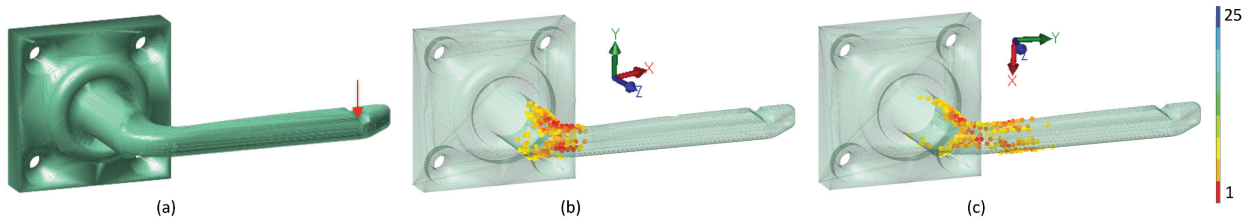

Fig. 6. Performance of our objective function. (a) Problem configuration. Elements with the lowest 300 safety factor values are highlighted for the initial (b), and the optimized (c), build orientations.

VeroWhite^{TM}photosensitive resin. For each specimen, we conduct a tensile test using an INSTRON 4467 instrument and two strain gauges mounted to the front and back faces of the specimen to obtain the engineering stress-strain curves for each specimen.

Figure 5(a) and (b) show the stress-strain curves for the three identical specimens printed along directions 2 and 5 (see Fig. 4(a)), respectively. The results show that the stress-strain curves of similarly oriented specimens behave similarly up to their ultimate tensile strength. Indeed, the deviation in the elastic moduli and yield strength values are less than 3%. Thus, the material properties are consistent within a given orientation. On the other hand, when the parts are printed in different directions, significant differences are observed in the material properties. Fig. 5(c) shows the stress-strain curves for the specimens printed in the seven different directions revealing the directional dependency of material properties.

We extract the material properties required for our optimization algorithm from the stress-strain curves. To this end, the Young's moduli and tensile yield strengths (0.2% strain offset) as well as the Poisson's ratios (the ratio between the slopes of the stress-axial strain and stress-transverse strain) are obtained for the directions of 1, 6, and 7 shown in Fig. 4(a). These directions correspond to our standardized principal directions and are listed in Tab. 1. Furthermore, we perform compression tests on the standard test specimens (ASTM D395) using an INSTRON 4469 compression instrument to obtain the compressive yield strengths shown in Tab. 1. For the orthotropic material model, it is also necessary to determine the shear related material properties. For this, we calculate the required shear moduli using the approach in [27]. The corresponding shear strengths are assumed to be 50% of the lowest yield strength value according to the maximum shear theory [35] for conservative estimates. However, shear strengths can also be experimentally determined to enhance the precision of our approach without loss of generality.

4 Build Orientation Selection

We quantify the structural robustness of an object using the factor of safety (FS) criterion. The overall goal is to choose a build orientation that maximizes the FS over the entire geometry.

For each element i, each FE simulation computes a stress tensor $\boldsymbol{\sigma}_i$ containing six unique components:

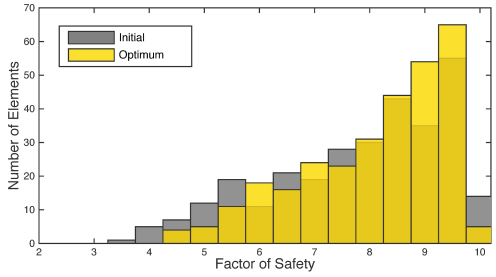

Fig. 7. Histograms of the lowest 300 FS values for the initial and optimized problem configurations of Fig. 6. Note the improvement in the minimum FS, as well as the general shift towards the right.

σ_X^i, σ_Y^i, σ_Z^i, τ_{YZ}^i, τ_{XZ}^i and τ_{XY}^i. Here, σ_m^i and τ_{mn}^i terms are the normal and shear stresses, respectively. Based on the maximum stress theory, a conservative approach to assign a single FS to an element is to compute six independent FS values for each stress component and choose the minimum one as the FS for that element. In our approach, we use this principle to formulate our optimization problem as follows:

$$\begin{aligned} \underset{\mathbf{x}}{\text{minimize}} \quad & f(\mathbf{x}) = \sum_{i=1}^{n} \left[\sum_{k=1}^{6} \left(\frac{1}{\mathbf{FS}_i^k(\mathbf{x})} \right)^{\kappa} \right] \\ \text{subject to} \quad & \alpha, \gamma \in [-\pi,\, \pi] \text{ and } \beta \in [0,\, \pi], \\ \text{where} \quad & \mathbf{x} = [\alpha, \beta, \gamma]^T. \end{aligned} \tag{1}$$

Here, $\mathbf{FS}_i$ is the 6×1 vector of safety factor values ($\mathbf{FS}_i^k$) for the i'th element, and $\mathbf{x}$ is the vector of design variables where α, β and γ are the intrinsic Euler angles representing a sequential rotation about the global z, x and z axes, respectively. κ is a large positive number and n is the number of elements in the FE analysis. The goal is to find $\mathbf{x}$ that minimizes our objective $f(\mathbf{x})$. In our approach, we calculate $\mathbf{FS}_i(\mathbf{x})$ for an element as follows:

$$\mathbf{FS}_i(\mathbf{x}) = \boldsymbol{\sigma}^{\boldsymbol{Y}} / \boldsymbol{\sigma}_{\mathbf{i}}'(\mathbf{x}) \;\text{ where }\; \boldsymbol{\sigma}_{\mathbf{i}}'(\mathbf{x}) = \mathbf{R}(\mathbf{x})\boldsymbol{\sigma}_{\mathbf{i}}\mathbf{R}^{\mathbf{T}}(\mathbf{x}) \tag{2}$$

where $\boldsymbol{\sigma}^{\boldsymbol{Y}}$ is the 6×1 vector of yield strengths for the anisotropic material obtained for the principal directions (material coordinates). $\boldsymbol{\sigma}_i$ is the stress tensor in the geometry

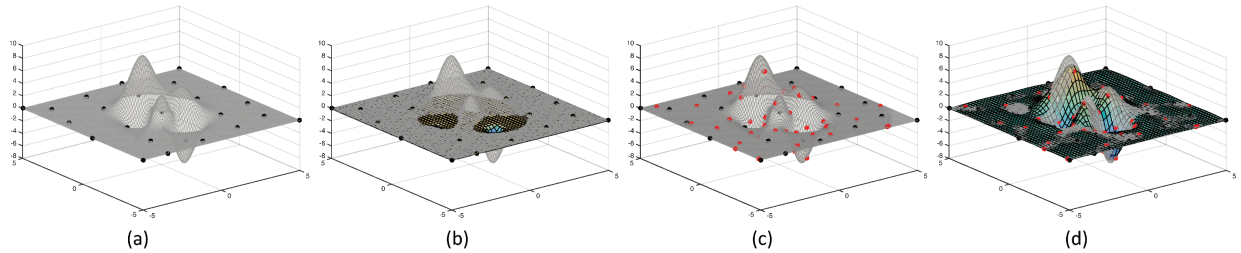

Fig. 8. (a) Initial design of experiments, (b) constructing a surrogate model, (c) selecting new samples and (d) enhancing the surrogate model. (b) and (c) are repeated until a certain stopping criteria is satisfied. Black and red dots represent initial and new samples, respectively. Transparent surface is the exact objective function and colored surface is the surrogate model constructed with the selected samples.

coordinates and $\boldsymbol{\sigma}_i'(\mathbf{x})$ is its transformation to the material coordinates. $\mathbf{R}(\mathbf{x})$ is the transformation matrix from geometry to material coordinates.

One advantage of our formulation given in Eqn. (1) is that the elements with lower FS values contribute more heavily to the objective function compared to those with high FS values. Hence, in each iteration, the optimization desirably focuses more on increasing the FS of the most critical elements. Figure 6 illustrates the performance of our objective function. For the given door handle, the FS for the most critical element is increased from 3.5 to 4.6 using our approach. Figure 7 shows the histograms of the lowest 300 FS values for the problem configuration shown in Fig. 6. As the orientation is optimized, the number of elements with low FS values decreases and the distribution shifts to the right.

5 Surrogate-based Optimization

Because our objective function is based on the stress values obtained from an FE analysis applied for each candidate orientation, finding the optimum orientation can be very expensive using conventional methods due to the large number simulations. This effort can be even more prohibitive for complex geometries with a large number of elements. Hence, it is critical to determine useful evaluation points to restrict the number of FE runs as much as possible. To address this challenge, we employ a surrogate modeling approach that approximates the design space with a proxy response surface.

Surrogate models (metamodels) are commonly used in engineering and design optimization when each function evaluation involves costly simulations [36–38]. In design optimization, these expensive objective functions or constraints are replaced with surrogate models that serve as approximations to the original functions.

We use surrogate modeling to approximate the design space represented by the build orientation $\mathbf{x}$ and the corresponding objective function $f(\mathbf{x})$ in Eqn. (1). This objective function is highly dependent on the geometry, loading configuration and orthotropic material properties, with no access to an analytical relationship between the design variables and the objective function. In all the examples presented in this paper, we have applied a brute force parametric sweeping as a benchmark and have found the resulting objective functions to be non-convex. We thus formulate our problem as a black-box global approximation problem and employ a surrogate-based optimization method. Specifically, we use MATLAB's Surrogate Model Toolbox (MATSuMoTo) presented in [39].

The main steps are as follows:

1. *Design of Experiments*: Select the number of initial orientations ($\mathbf{x}$'s) and evaluate the corresponding objective functions ($f(\mathbf{x})$'s) using FE simulations.
2. *Surrogate Modeling*: Construct the surrogate model mapping $\mathbf{x}$'s to $f(\mathbf{x})$'s.
3. *New Samples*: Select new samples using the surrogate model and perform new FE simulations.
4. *Iterate*: Iterate until the maximum number of function evaluations is reached or the improvement $f(\mathbf{x})$ ceases.

Figure 8 shows an example for a two dimensional problem. The third dimension shows the objective values. Here, the transparent surface represents the exact values of the objective function in the specified design space. As the number of iterations (*i.e.,* the number of samples evaluated using the expensive objective function) increases, the surrogate model converges to the exact values of the objective function.

In Step 1, in order to determine the initial orientations, we use the Latin hypercube sampling (LHS) method with 'maximin' criterion that allows a wider and more uniform coverage of the design space by maximizing the pairwise distances between the sample points. This is a statistical method commonly used for design of experiments. Because there is no a priori information about the design space, LHS is a suitable method that spreads the sample points evenly across the design space. In order to evaluate the objective function at the selected orientations, we use ANSYS Mechanical APDL, and obtain the stress tensor field and calculate the FS values using Eqn. (2).

For surrogate modeling, there are several methods available in the literature including polynomial regression models [40], radial basis functions (RBF) [41–43], neural networks [44], kriging [36, 45] and support vector machines [46]. The best choice for the surrogate modeling method is usually problem dependent. In this paper, we use a cubic RBF (with leave-one-out cross validation) to construct the surrogate model because of its simplicity, robustness to different problem settings and high performance for small sample sizes [47]. However, it is possible to use other

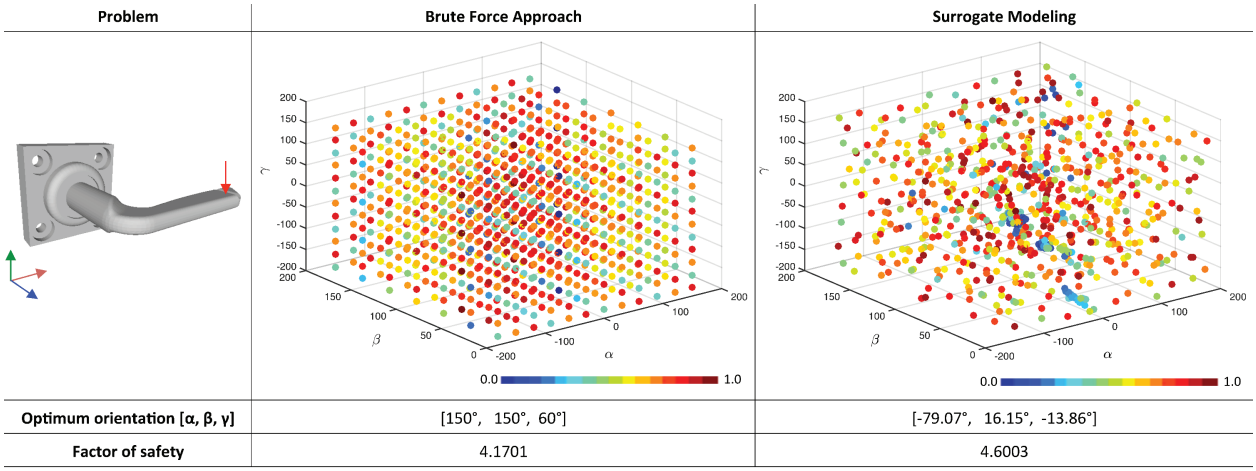

Fig. 9. Comparison of surrogate-based optimization with brute force approach. Samples representing different build orientations are shown with dots. The color of each dot represents the normalized objective function value for the corresponding orientation. The best orientations obtained with the two methods and the corresponding minimum FS values are also shown.

methods or combinations based on the problem setup and the characteristics of the design space, if known apriori. Comparative studies addressing this challenge can be found in the literature [47–49]. In Step 3, the constructed surrogate model is used to approximate the objective function in the remainder of the design space without performing costly FE simulations. For the next iteration, we use the randomized global candidate point search as our sampling strategy. Here, in addition to the set of candidate points around the minimum of the surrogate model, a number of uniformly distributed samples are selected across the entire domain. We choose this strategy to avoid possible local minima.

Figure 9 compares our surrogate based optimization with the brute force approach of uniformly sampling the design space. Here, 1008 objective function evaluations are performed using both the brute force and the surrogate-based approaches hence making the computational effort identical in both cases. This number represents a uniform grid of 30 degree increments in each of the design variables in the brute force method. With the surrogate-based optimization, the minimum FS obtained for the optimum orientation after 1008 function evaluations is approximately 10% better than that computed by the brute force approach. It can also be observed that the surrogate modeling enables a more efficient sampling strategy where regions of local minima are more rigorously explored (dense regions with many blue points in Fig. 9).

Figure 10 illustrates the performance of the surrogate modeling approach as a function of evaluation points for the problem shown in Fig. 9. It can be observed that using only 215 function evaluations, the surrogate model can attain the best FS computed by the brute force approach which uses 1008 samples. Although the numerical values here might be problem dependent and may vary, similar gains are expected to be observed for various problem settings.

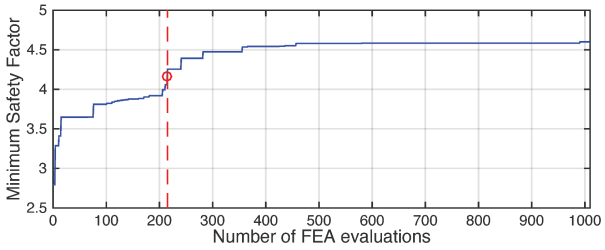

Fig. 10. Performance of surrogate-based optimization for problem configuration in Fig. 9 with respect to the sample size. Red circle shows the best objective value that can be obtained using the brute force approach. With surrogate-based optimization, the same performance level of brute force approach can be obtained with only 215 samples.

6 Results and Discussion

For a fixed geometry and material, the optimum build orientation may change drastically if the loading configuration changes. In Fig. 11, optimum orientations are investigated for two different loading configurations of the door handle (displacement boundary conditions are kept the same). It can be observed that the difference between the optimal build orientations for these two examples is quite distinct.

Figure 12 demonstrates the proposed algorithm on different problems. In all cases, we observed significant improvements in the FS when our optimization approach is applied. Table 2 shows the improvement in FS for several problem configurations. Depending on the geometry, loading, boundary conditions and the initial orientation, we were able to achieve up to 90% improvement in the resulting FS values. It is also important to note that in some examples (such as the slingshot and the nut cracker), it is possible to move from unsafe ($FS < 1.0$) to safe ($FS > 1.0$) using our method without any geometric modification.

Table 3 shows the computational performance of our ap-

Table 2. Numerical results for several test cases.

Problem Setup	Optimum Orientation	Initial FS	Optimum FS	% Improvement
Door Handle (Fig. 11-Top)	$[-79.07°, 16.15°, -13.86°]$	3.3202	4.6003	38.55
Door Handle (Fig. 11-Bottom)	$[117.10°, 26.19°, -180°]$	1.6881	2.2259	31.85
Spring (Fig. 12)	$[56.12°, 35.25°, -5.33°]$	9.7441	12.0901	24.07
Slingshot (Fig. 12)	$[-100.12°, 128.06°, 179.01°]$	0.9123	1.2056	32.15
Nut Cracker (Fig. 12)	$[7.80°, 123.97°, -93.32°]$	0.7815	1.4844	89.94

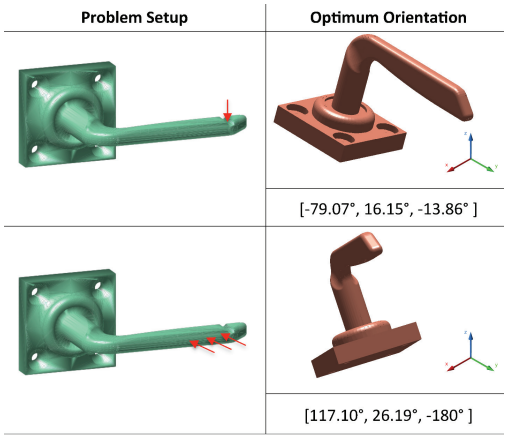

Fig. 11. Effect of different loading configurations on the optimum build orientation. Left column shows the problem configuration and right column shows the corresponding optimum build orientations.

Table 3. Computational performance of our method for several test cases. The maximum number of objective function evaluations are limited to 400.

Problem Setup	Number of FEA Elements	Computation Time [s]
Door Handle (Fig. 11)	11290	1196.3999
Spring (Fig. 12)	94228	5571.1827
Slingshot (Fig. 12)	37558	2655.4636
Nut Cracker (Fig. 12)	9145	1124.9073

proach for problems with different mesh complexities. Because the FE simulations constitute the computational bottleneck, the number of elements directly impact the overall computation time. We observe that the computation time per element is similar for all models and it is approximately $0.1s$. In these problems, the stopping criterion is the maximum number of objective evaluations (*i.e.,* FE simulations) which is selected to be 400. A PC with a 2.4GHz Core CPU and 8GB RAM using MATLAB R2014b is used for surrogate modeling, which drives the FE simulations using a script based ANSYS Mechanical APDL (v14).

We conducted two sets of physical experiments to evaluate the performance of our approach. First, for the seven orientations shown in Fig. 4(a), we computationally determined the best orientation by calculating our objective function for each of the orientations. Direction 2 proved to be the best orientation. For the same geometry and loading configuration, we then computed the optimum orientation using the proposed surrogate modeling approach, printed a new specimen corresponding to this optimum orientation, and conducted a tensile test. Figure 13 compares the stress-strain curves for these two orientations. It is observed that our optimum orientation improves the yield strength by 13% (from 40.14 MPa to 45.56 MPa).

We conducted another test on a custom-designed part shown in Fig. 14. Note that aside from the conventional tensile specimens, there are not many design alternatives to physically observe and quantify yielding. As a result, we devised an experiment where we simultaneously acquire the forces and the elongation using a tensile-test machine. We compare the orientation we obtained with our approach against the orientation that minimizes the amount of support structure (machine orientation) and an orientation based on a mechanical engineer's best judgement (Fig. 14). It is shown that our optimized orientation withstands a higher end force before yielding compared to the other two directions (12% and 20% better compared to human and machine prediction, respectively). For each of the model and loading configuration shown in this paper, we asked several engineers to predict the best orientation to maximize FS. In all cases, our approach outperformed human judgment.

Scope and assumptions: Our analysis is restricted to homogeneous materials and we assume a linear-elastic FE model to successfully simulate the stress and strains in the object. Our failure criteria is based on maximum stresses and we do not consider strain failure or maximum displacement constraints. However, since our approach is based on FE simulations, it is readily possible to include such criteria in the objective function or the constraints without loss of generality. The yield criterion we use is accurately applicable to ductile materials. For brittle materials, we use the ultimate tensile strength (UTS) as the yield strength. This assumption may cause our analysis for brittle materials to be less accurate compared to ductile materials.

Our approach assumes that the properties extracted from the tensile test specimens accurately represent the properties of the designed object. In certain printing techniques such as FDM, each layer may involve first a contouring of the layer where the outline of the layer is printed, followed by a raster fill-in. In such cases, the properties will be a function of the object's scale, thus possibly creating a mismatch between the test specimen's and the actual object's proper-

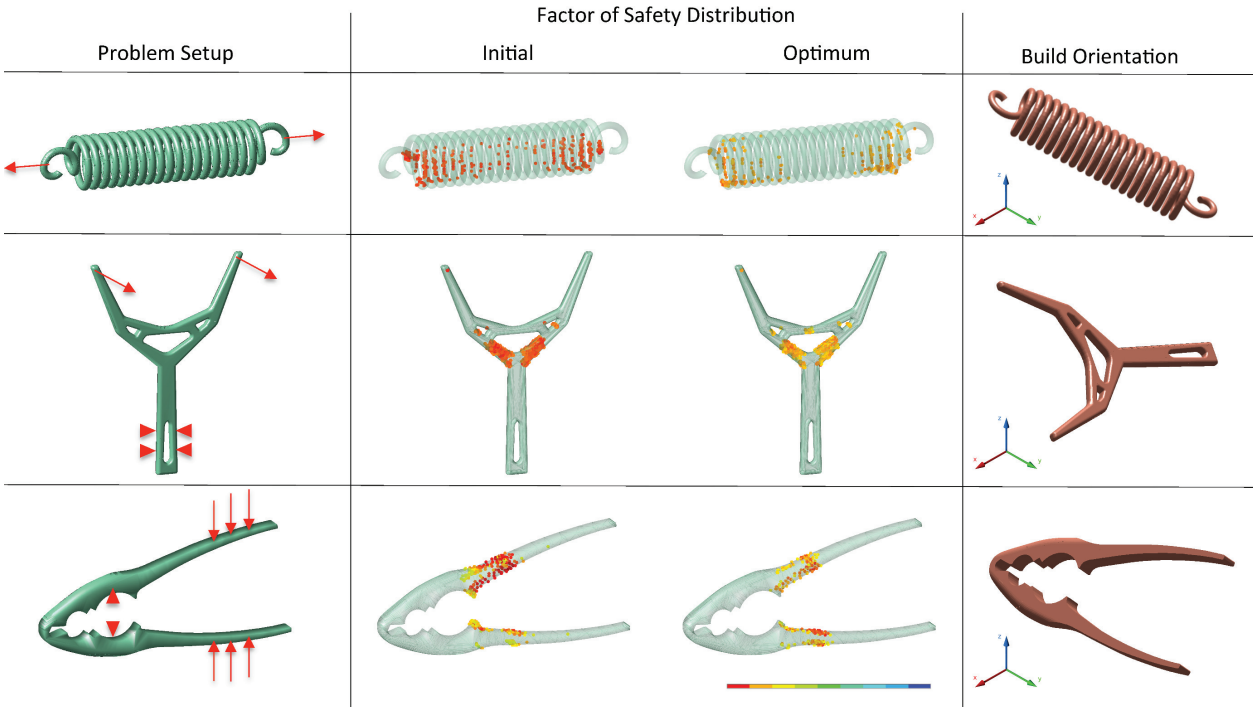

Fig. 12. Build orientation optimization results for three different problem configurations. Left column shows the problem settings. Middle column shows the distribution of the lowest 300 FS values over the geometry for the initial and optimum orientations. Right column shows the optimum build orientations.

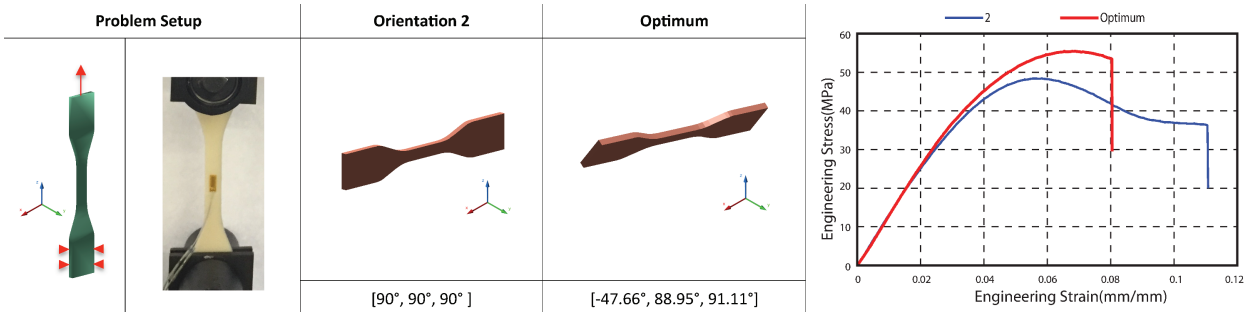

Fig. 13. Performance evaluation of our algorithm with a standard dog-bone tensile specimen.

ties. Also, we assume that the effects of support structure on the anisotropic mechanical properties of fabricated products are negligible. However, investigation and incorporation of these effects might enhance the performance of the presented method further.

7 Conclusions

Additively manufactured products exhibit directional dependencies in their structural properties due to the layered nature of the printing process. As a result, the build orientation can significantly affect the structural performance of the resulting objects. In this paper, we developed a build orientation optimization algorithm that maximizes the mechanical strength of an additively manufactured object under certain loading/boundary configurations. We start with a set of physical experiments to determine the orthotropic material properties. Then, our optimization approach uses this information to calculate an optimum build orientation.

Our objective in the optimization problem is formulated based on the factor of safety values obtained using FE simulations. We have shown that a surrogate-based optimization approach can accelerate the optimization process by strategically choosing useful evaluations points. Both our computational and physical experiments show that the optimized build direction can lead to considerable improvements in an object's ability to withstand applied loads.

Future work: In this work, we explored our build orientation optimization algorithm only for a single polymer material and AM process combination. We expect the proposed formulation to be readily applicable to new polymer-based materials and print technologies. While we have observed a strong consistency among the samples printed in the same orientation, more studies quantifying the sensitivity of the results to the process parameters may be required to further

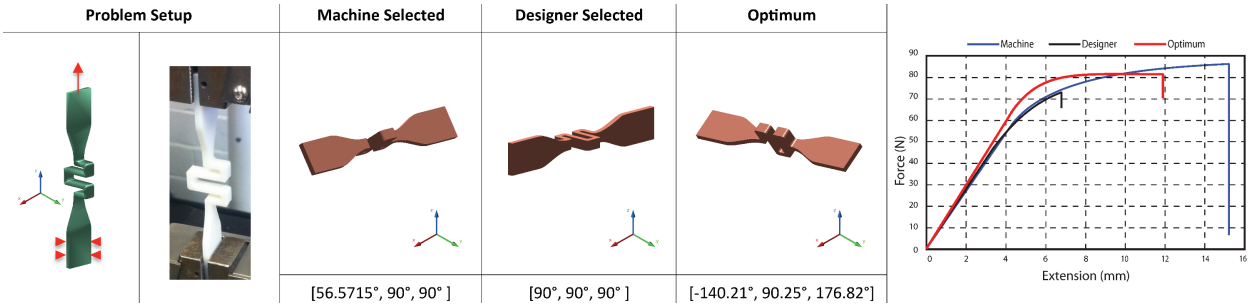

Fig. 14. Performance evaluation of our algorithm with a custom-designed part.

validate the proposed work. We have not tested the proposed method to AM of metals. Recent efforts in process and microstructural modeling/simulation for metals would be critical for a successful extension of the proposed method to metals. Our preliminary discussions reveal that there may be a large number of parameters that affect anisotropy making such properties a strong function of the overall part geometry, spatial position in the print volume, thermal aspects of the process and post processes applied to the part. Moreover, in this work, we optimize the build orientation for a single loading configuration only. Yet, the optimization problem can be extended to ensure that the resulting build orientation is robust to multiple different loading configurations. This may require solving the problem multiple times using different loading configurations and choosing an orientation that jointly maximizes the FS for all considered loading conditions. Likewise, the uncertainty on the loading conditions could be encoded statistically to solve for a more robust build orientation. Finally, other criteria such as creep and fatigue failure provide interesting research opportunities for build direction optimization.

References

[1] Campbell, T., Williams, C., Ivanova, O., and Garrett, B., 2011. "Could 3d printing change the world". *Technologies, Potential, and Implications of Additive Manufacturing, Atlantic Council, Washington, DC*.

[2] Vaezi, M., Seitz, H., and Yang, S., 2013. "A review on 3d micro-additive manufacturing technologies". *The International Journal of Advanced Manufacturing Technology,* **67**(5-8), pp. 1721–1754.

[3] Scott, J., Gupta, N., Weber, C., Newsome, S., Wohlers, T., and Caffrey, T., 2012. "Additive manufacturing: status and opportunities". *Science and Technology Policy Institute, Washington, DC*, pp. 1–29.

[4] Gibson, I., Rosen, D. W., and Stucker, B., 2009. *Additive Manufacturing Technologies: Rapid Prototyping to Direct Digital Manufacturing*, 1st ed. Springer Publishing Company, Incorporated.

[5] Seepersad, C. C., 2014. "Challenges and opportunities in design for additive manufacturing". *3D Printing and Additive Manufacturing,* **1**(1), pp. 10–13.

[6] Lipson, H., and Kurman, M., 2013. *Fabricated: The new world of 3D printing*. John Wiley & Sons.

[7] Bickel, B., Bächer, M., Otaduy, M. A., Lee, H. R., Pfister, H., Gross, M., and Matusik, W., 2010. "Design and fabrication of materials with desired deformation behavior". *ACM Trans. Graph.,* **29**(4), July.

[8] Chen, D., Levin, D. I. W., Didyk, P., Sitthi-Amorn, P., and Matusik, W., 2013. "Spec2fab: A reducer-tuner model for translating specifications to 3d prints". *ACM Trans. Graph.,* **32**(4), July, pp. 135:1–135:10.

[9] Hašan, M., Fuchs, M., Matusik, W., Pfister, H., and Rusinkiewicz, S., 2010. "Physical reproduction of materials with specified subsurface scattering". *ACM Trans. Graph.,* **29**(4), July, pp. 61:1–61:10.

[10] Dong, Y., Wang, J., Pellacini, F., Tong, X., and Guo, B., 2010. "Fabricating spatially-varying subsurface scattering". *ACM Trans. Graph.,* **29**(4), July, pp. 62:1–62:10.

[11] Prévost, R., Whiting, E., Lefebvre, S., and Sorkine-Hornung, O., 2013. "Make it stand: Balancing shapes for 3d fabrication". *ACM Trans. Graph.,* **32**(4), July, pp. 81:1–81:10.

[12] Bächer, M., Whiting, E., Bickel, B., and Sorkine-Hornung, O., 2014. "Spin-it: Optimizing moment of inertia for spinnable objects". *ACM Trans. Graph.,* **33**(4), July, pp. 96:1–96:10.

[13] Alexander, P., Allen, S., and Dutta, D., 1998. "Part orientation and build cost determination in layered manufacturing". *Computer-Aided Design,* **30**(5), pp. 343 – 356.

[14] Xu, F., Loh, H., and Wong, Y., 1999. "Considerations and selection of optimal orientation for different rapid prototyping systems". *Rapid Prototyping Journal,* **5**(2), pp. 54–60.

[15] Ahn, D., Kim, H., and Lee, S., 2007. "Fabrication direction optimization to minimize post-machining in layered manufacturing". *International Journal of Machine Tools and Manufacture,* **47**(3-4), pp. 593 – 606.

[16] Canellidis, V., Giannatsis, J., and Dedoussis, V., 2009. "Genetic-algorithm-based multi-objective optimization of the build orientation in stereolithography". *The International Journal of Advanced Manufacturing Technology,* **45**(7-8), pp. 714–730.

[17] Thrimurthulu, K., Pandey, P. M., and Reddy, N. V., 2004. "Optimum part deposition orientation in fused deposition modeling". *International Journal of Machine Tools and Manufacture,* **44**(6), pp. 585 – 594.

[18] Vanek, J., Galicia, J. A. G., and Benes, B., 2014. "Clever support: Efficient support structure generation for digital fabrication". *Computer Graphics Forum,* **33**(5), pp. 117–125.

[19] Ahn, S.-H., Montero, M., Odell, D., Roundy, S., and Wright, P. K., 2002. "Anisotropic material properties of fused deposition modeling abs". *Rapid Prototyping Journal,* **8**(4), pp. 248–257.

[20] Bagsik, A., and Schöppner, V., 2011. "Mechanical properties of fused deposition modeling parts manufactured with ultem* 9085". *ANTEC 2011*.

[21] El-Gizawy, A. S., Corl, S., and Graybill, B., 2011. "Process-induced properties of fdm products". In Proceedings of The ICMET.

[22] Hill, N., and Haghi, M., 2014. "Deposition direction-dependent failure criteria for fused deposition modeling polycarbonate". *Rapid Prototyping Journal,* **20**(3), pp. 221–227.

[23] Barclift, M. W., and Williams, C. B., 2012. "Examining variability in the mechanical properties of parts manufactured via polyjet direct 3d printing". In International Solid Freeform Fabrication Symposium, August, pp. 6–8.

[24] Kesy, A., and Kotliński, J., 2010. "Mechanical properties of parts produced by using polymer jetting technology". *Archives of civil and mechanical engineering,* **10**(3), pp. 37–50.

[25] Galeta, T., Kladaric, I., and Karakasic, M., 2013. "Influence of processing factors on the tensile strength of 3d-printed models". *Material Technology (MTAEC9),* **47**(6), pp. 781–788.

[26] Hildebrand, K., Bickel, B., and Alexa, M., 2013. "Orthogonal slicing for additive manufacturing". *Computers and Graphics,* **37**(6), pp. 669 – 675.

[27] Zhou, Q., Panetta, J., and Zorin, D., 2013. "Worst-case structural analysis". *ACM Trans. Graph.,* **32**(4), July, pp. 137:1–137:12.

[28] Umetani, N., and Schmidt, R., 2013. "Cross-sectional structural analysis for 3d printing optimization". In SIGGRAPH Asia 2013 Technical Briefs, SA '13, ACM, pp. 5:1–5:4.

[29] Luo, L., Baran, I., Rusinkiewicz, S., and Matusik, W., 2012. "Chopper: Partitioning models into 3d-printable parts". *ACM Trans. Graph.,* **31**(6), Nov., pp. 129:1–129:9.

[30] Stava, O., Vanek, J., Benes, B., Carr, N., and Měch, R., 2012. "Stress relief: Improving structural strength of 3d printable objects". *ACM Trans. Graph.,* **31**(4), July, pp. 48:1–48:11.

[31] Wang, W., Wang, T. Y., Yang, Z., Liu, L., Tong, X., Tong, W., Deng, J., Chen, F., and Liu, X., 2013. "Cost-effective printing of 3d objects with skin-frame structures". *ACM Trans. Graph.,* **32**(6), Nov., pp. 177:1–177:10.

[32] Lu, L., Sharf, A., Zhao, H., Wei, Y., Fan, Q., Chen, X., Savoye, Y., Tu, C., Cohen-Or, D., and Chen, B., 2014. "Build-to-last: Strength to weight 3d printed objects". *ACM Trans. Graph.,* **33**(4), July, pp. 97:1–97:10.

[33] Suh, Y. S., and Wozny, M. J., 1995. "Integration of a solid freeform fabrication process into a feature-based CAD system environment". In Solid Freeform Fabrication Symposium, H. L. M. et al., ed.

[34] Thompson, D. C., and Crawford, R. H., 1995. "Optimizing part quality with orientation". In Proceedings of the Solid Freeform Fabrication Symposium, Vol. 6, pp. 362–368.

[35] Shigley, J. E., Budynas, R. G., and Mischke, C. R., 2004. *Mechanical engineering design*. McGraw-Hill.

[36] Simpson, T. W., Mauery, T. M., Korte, J. J., and Mistree, F., 2001. "Kriging models for global approximation in simulation-based multidisciplinary design optimization". *AIAA journal,* **39**(12), pp. 2233–2241.

[37] Queipo, N. V., Haftka, R. T., Shyy, W., Goel, T., Vaidyanathan, R., and Tucker, P. K., 2005. "Surrogate-based analysis and optimization". *Progress in Aerospace Sciences,* **41**(1), pp. 1 – 28.

[38] Wang, G. G., and Shan, S., 2007. "Review of metamodeling techniques in support of engineering design optimization". *Journal of Mechanical Design,* **129**(4), pp. 370–380.

[39] Mueller, J., 2014. "Matsumoto: The matlab surrogate model toolbox for computationally expensive black-box global optimization problems". *arXiv preprint arXiv:1404.4261*.

[40] Myers, R. H., and Montgomery, D. C., 1995. *Response Surface Methodology: Process and Product in Optimization Using Designed Experiments*, 1st ed. John Wiley & Sons, Inc., New York, NY, USA.

[41] Simpson, T., Poplinski, J., Koch, P. N., and Allen, J., 2001. "Metamodels for computer-based engineering design: Survey and recommendations". *Engineering with Computers,* **17**(2), pp. 129–150.

[42] Powell, M. J., 1990. *The theory of radial basis function approximation in 1990*. University of Cambridge. Department of Applied Mathematics and Theoretical Physics.

[43] Mullur, A. A., and Messac, A., 2005. "Extended radial basis functions: more flexible and effective metamodeling". *AIAA journal,* **43**(6), pp. 1306–1315.

[44] Haykin, S., 1999. *Neural Networks: A Comprehensive Foundation*. Prentice-Hall.

[45] Martin, J. D., and Simpson, T. W., 2004. "On the use of kriging models to approximate deterministic computer models". In International Design Engineering Technical Conferences and Computers and Information in Engineering Conference, American Society of Mechanical Engineers, pp. 481–492.

[46] Girosi, F., 1998. "An equivalence between sparse approximation and support vector machines". *Neural computation,* **10**(6), pp. 1455–1480.

[47] Jin, R., Chen, W., and Simpson, T. W., 2001. "Comparative studies of metamodelling techniques under multiple modelling criteria". *Structural and Multidisciplinary Optimization,* **23**(1), pp. 1–13.

[48] Muller, J., and Shoemaker, C. A., 2014. "Influence of ensemble surrogate models and sampling strategy on

the solution quality of algorithms for computationally expensive black-box global optimization problems". *Journal of Global Optimization,* **60**(2), pp. 123–144.

[49] Mullur, A. A., and Messac, A., 2006. "Metamodeling using extended radial basis functions: a comparative approach". *Engineering with Computers,* **21**(3), pp. 203–217.